A strategy for scaling up the Fischer–Tropsch bubble column slurry reactor

R. Krishna* and J.M. van Baten

Department of Chemical Engineering, University of Amsterdam, Nieuwe Achtergracht 166, 1018 WV Amsterdam, The Netherlands

For successful scale-up of the bubble column slurry reactor for Fischer–Tropsch synthesis, we need to have proper description of hydrodynamics and transport phenomena (gas and liquid holdups, liquid-phase residence time distribution, gas–liquid mass transfer, heat transfer to cooling tubes) as a function of reactor scale (column diameter and height) and operating conditions (superficial gas velocity, system pressure, slurry concentration, . . .). We discuss and develop a scale-up strategy using computational fluid dynamics, with a minimum amount of experimental input from hydrodynamic studies carried out on a relatively small scale.

KEY WORDS: gas holdup; bubble columns; scale effects; computational fluid dynamics; liquid circulations; concentrated slurries.

1. Introduction

The Fischer–Tropsch reaction that was discovered in Germany nearly three-quarters of a century ago has recently become a subject of renewed interest, particularly in the context of the conversion of remote natural gas to liquid transportation fuels. For economic and logistic reasons, such conversions are best carried out in large-scale projects, and the capability of up-scaling is therefore an important consideration in the selection of reactors for synthesis gas generation as well as in Fischer–Tropsch synthesis. It is now widely accepted that the bubble column slurry reactor is the best choice of reactor type for large-scale plants with capacities of the order of 40 000 bbl/day. Typical design and operating conditions of a Fischer–Tropsch slurry bubble column diameter for an optimally designed reactor can be obtained from the information given by Maretto and Krishna [1]:

- The column diameter ranges from 6–10 m.
- The column height is in the range of 30–40 m.
- The reactor operates at a pressure of between 3 and 5 Mpa.
- The reactor temperature is about 513–523 K.
- The superficial gas velocity is in the range 0.10–0.4 m/s, depending on the catalyst activity and the catalyst concentration in the slurry phase.
- For high reactor productivities, the highest slurry concentrations consistent with catalyst handleability should be used. In practice, the volume fraction of catalyst in the slurry phase, ε_s, is in the range 0.3–0.4.
- For removing the heat of reaction, 5000–8000 vertical cooling tubes, say of 50-mm diameter and 150-mm pitch, will need to be installed in a reactor of, say, 6 m.

* To whom correspondence should be addressed.
E-mail: krishna@science.uva.nl

The success of the process largely depends on the ability to achieve deep syngas conversions, say, exceeding 95%. Reliable design of the reactor to achieve such high conversion levels requires reasonably accurate information on the following hydrodynamics and mass transfer parameters:

- Gas holdup.
- Interphase mass transfer between the gas bubbles and the slurry.
- Axial dispersion of the liquid (slurry) phase.
- Axial dispersion of the gas phase.
- Heat transfer coefficient to cooling tubes.

Most of the above-mentioned hydrodynamic parameters are interrelated. For a given column diameter, the bubble rise velocity affects the gas holdup and also determines the strength of the liquid circulations and, consequently, the axial dispersion coefficient of the liquid phase. The distribution of bubble sizes and rise velocities determines the axial dispersion coefficient of the gas phase. The heat transfer to the cooling tubes is influenced by the renewal rate of the liquid film on the tube surface, which in turn is dictated by the bubble rise velocity. Increasing the column diameter has the effect of increasing the liquid circulations, which enhances the bubble rise velocity; this impacts on all the hydrodynamic parameters. For a proper description of the hydrodynamics at different scales, we make use of computational fluid dynamics (CFD) in the Eulerian framework; this technique has been applied with some success in the description of hydrodynamics of bubble column reactors [2–11]. In the CFD model developed in the present communication, the interphase momentum exchange or drag coefficient is obtained from experimental measurements on a relatively small scale.

In order to demonstrate our scale-up approach, we have carried out experimental studies on slurry bubble

1022-5528/03/1200–0021/0

columns in columns of 0.1, 0.19 and 0.38 m in diameter. These experimental results are compared with CFD simulations. Furthermore, we perform CFD simulations for a 6-m column to demonstrate the significant influence of scale on column hydrodynamics.

2. Experimental setup and results

Experiments were performed in polyacrylate columns with inner diameters of 0.1, 0.19 and 0.38 m. The gas distributors used in the three columns were all made of sintered bronze plate (with a mean pore size of 50 μm). The gas flow rates entering the column were measured with the use of a set of rotameters, placed in parallel, as shown in figure 1 for the 0.38-m column. This setup was typical. Air was used as the gas phase in all experiments. Firstly, experiments were performed with paraffin oil (density, $\rho_L = 790\,kg/m^3$; viscosity, $\mu_L = 0.0029\,Pa.s$; surface tension, $\sigma = 0.028\,N/m$) as liquid phase to which solid particles in varying concentrations were added. The solid phase used consisted of porous silica particles whose properties were determined to be as follows: skeleton density $= 2100\,kg/m^3$; pore volume $= 1.05\,mL/g$; particle size distribution, d_p: 10% $< 27\,\mu$m; 50% $< 38\,\mu$m; 90% $< 47\,\mu$m. The solids concentration, ε_s, is expressed as the volume fraction of solids in gas-free slurry. The pore volume of the particles (liquid filled during operation) is counted as being part of the solid phase. Further details of the experimental work is available in [3,4,9,12,13].

The influence of the solids concentration on the total gas holdup, ε, for varying superficial gas velocities are shown in figure 2 for the 0.38-m diameter column. It is observed that increased particles concentration tends to decrease the total gas holdup, ε, to a significant extent. This decrease in the total gas holdup is due to the decrease in the holdup of the small bubbles due to enhanced coalescence caused because of the presence of small particles. At low solid concentrations, there is a pronounced maximum in the gas holdup, which is typical of the transition region. With increased solids concentration, the transition occurs at a lower superficial gas velocity and the transition "window" reduces in size. Figure 3 presents a qualitative picture of the influence of gas velocity and particles concentration. At particles concentration exceeding 30 vol%, the dispersion consists almost exclusively of fast-rising large bubbles.

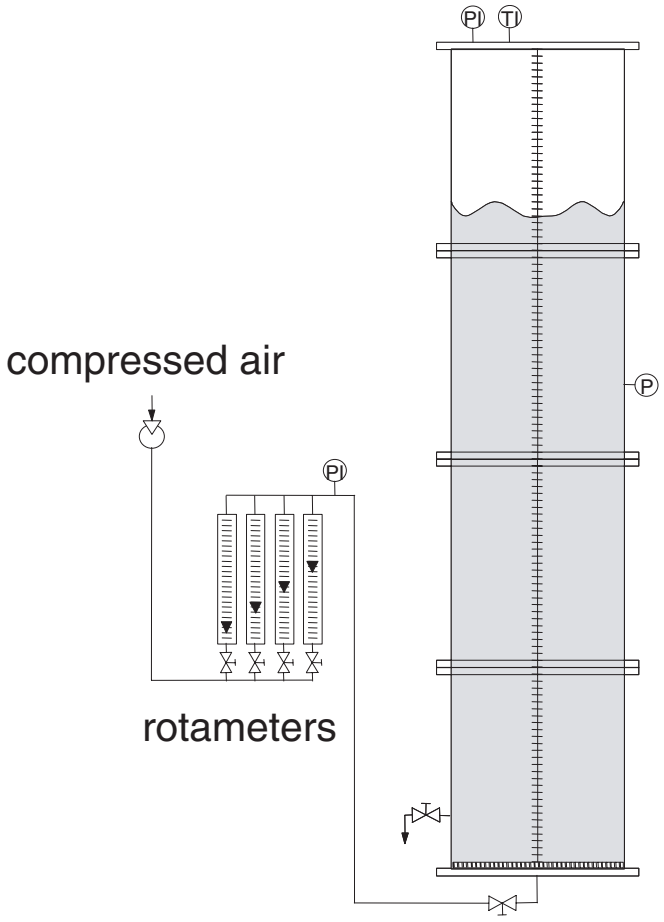

Figure 1. Typical experimental setup for the 0.38-m diameter column.

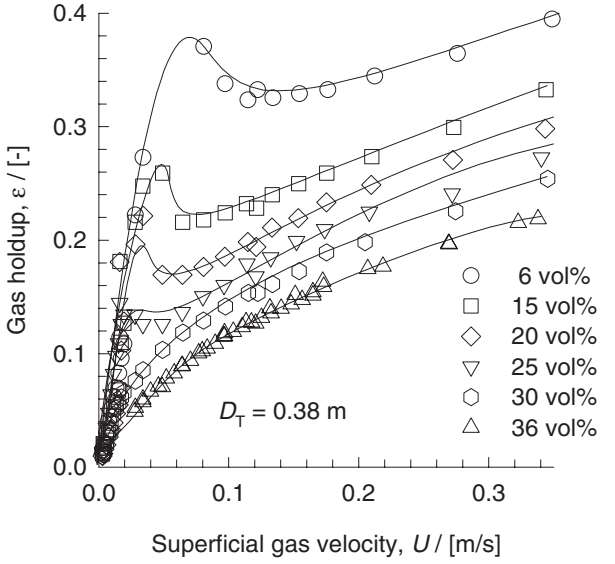

Figure 2. Influence of increased particles concentration on the total gas holdup in 0.38-m diameter column. The liquid phase is paraffin oil containing varying concentrations of silica particles.

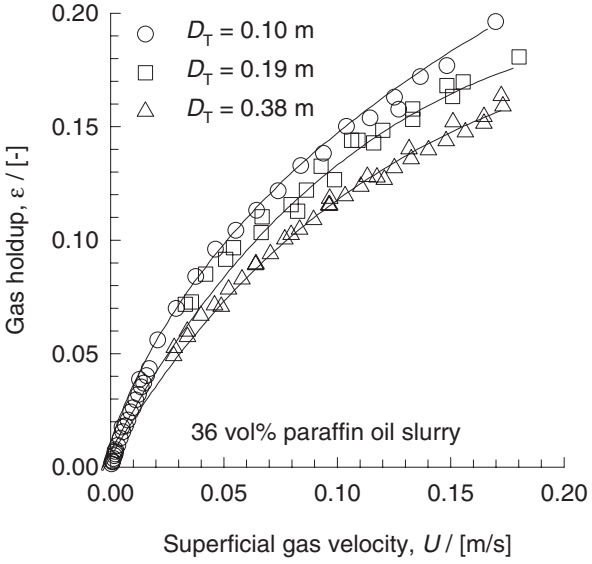

Figure 4. Influence of column diameter on the gas holdup in 36 vol% paraffin–oil slurry system.

For a slurry concentration of 36 vol%, the gas holdup decreases with column diameter; see figure 4. With increasing column diameter, the liquid circulation velocities are higher, with the consequence that the bubbles tend to be accelerated leading to lower gas holdup. This is evidenced by plotting the bubble swarm velocity, V_b, calculated from $V_b = U/\varepsilon$ for the three columns; see figure 5. At low superficial gas velocities, the bubble swarm velocity is practically the same for the three columns and $V_{b0} = 0.47$ m/s; this is indicated by the large filled circle in figure 5. The liquid circulations tend to accelerate the bubbles traveling upward in the central core. When the bubbles disengage at the top of the dispersion, the liquid travels back down the wall region. Clearly, to describe the influence of liquid circulations on the gas holdup, we need to be able to predict the liquid circulation velocity as a function of U and D_T. To enable such a prediction, we resort to Eulerian simulations of the bubble column hydrodynamics.

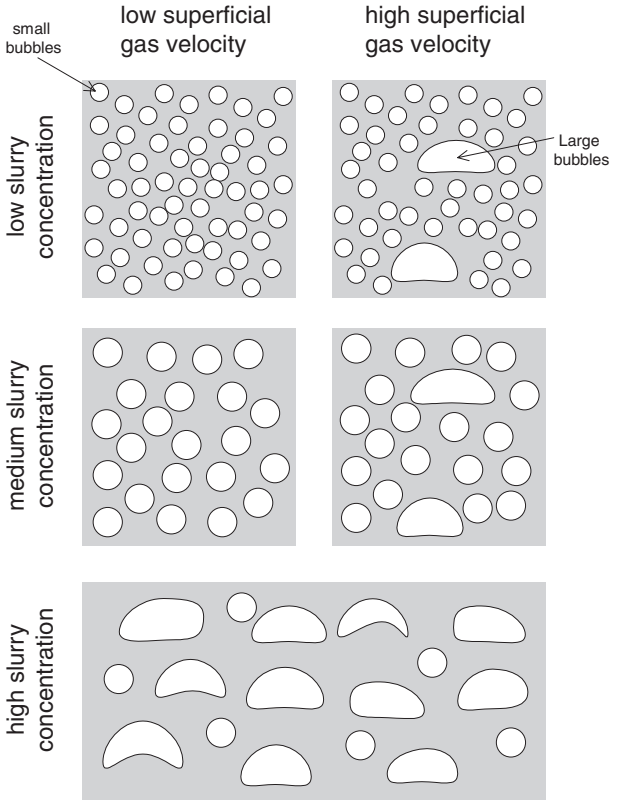

Figure 3. Qualitative picture of the influence of particles concentration and superficial gas velocity on bubble dispersions.

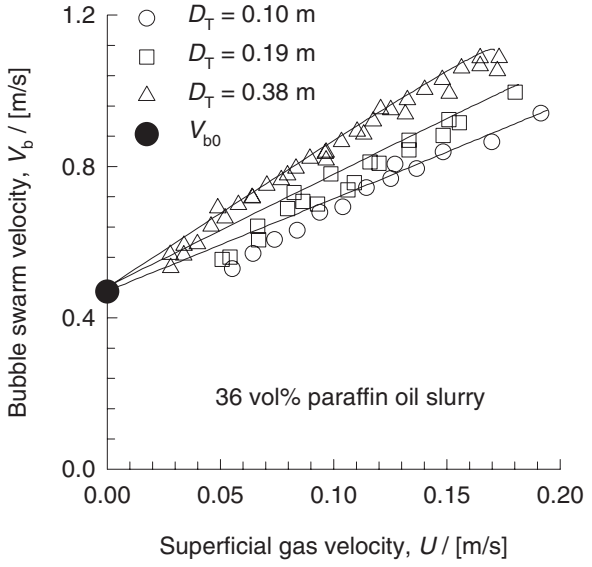

Figure 5. Influence of column diameter on the average bubble swarm velocity in 36 vol% paraffin–oil slurry system.

3. Development of Eulerian simulation model

For either gas or liquid phase, the volume-averaged mass and momentum conservation equations in the Eulerian framework are given by

$$\frac{\partial(\varepsilon_k\rho_k)}{\partial t} + \nabla \bullet (\rho_k\varepsilon_k\mathbf{u}_k) = 0 \quad (1)$$

$$\frac{\partial(\rho_k\varepsilon_k\mathbf{u}_k)}{\partial t} + \nabla \bullet \left(\rho_k\varepsilon_k\mathbf{u}_k\mathbf{u}_k - \mu_k\varepsilon_k\left(\nabla\mathbf{u}_k + (\nabla\mathbf{u}_k)^{\mathrm{T}}\right)\right) = -\varepsilon_k\nabla p + \mathbf{M}_{kl} + \rho_k\varepsilon_k\mathbf{g} \quad (2)$$

Here, ρ_k, $\mathbf{u}_k$, ε_k and μ_k represent respectively, the macroscopic density, velocity, volume fraction and viscosity of phase k, p is the pressure, $\mathbf{M}_{kl}$, the interphase momentum exchange between phase k and phase l and $\mathbf{g}$ is the gravitational force. On the basis of the hydrodynamic similarities between bubble columns operating with concentrated slurries and highly viscous liquids, we treat the slurry phase as a highly viscous liquid phase and use the properties of Tellus oil ($\rho_{\mathrm{L}} = 862$; $\mu_{\mathrm{L}} = 0.075$; $\sigma = 0.028$).

The momentum exchange between the gas phase (subscript G) and liquid phase (subscript L) is given by

$$\mathbf{M}_{\mathrm{L,G}} = \left[\frac{3}{4}\frac{C_{\mathrm{D}}}{d_{\mathrm{b}}}\rho_{\mathrm{L}}\right]\varepsilon_{\mathrm{G}}\varepsilon_{\mathrm{L}}(\mathbf{u}_{\mathrm{G}} - \mathbf{u}_{\mathrm{L}})|\mathbf{u}_{\mathrm{G}} - \mathbf{u}_{\mathrm{L}}| \quad (3)$$

where we follow the formulation given by Pan *et al*. [14]. We have only included the drag force contribution to $\mathbf{M}_{\mathrm{L,G}}$, in keeping with the works of Sanyal *et al*. [15] and Sokolichin & Eigenberger [16]. The added mass and lift-force contributions were both ignored in the present analysis. We propose the following relation for the estimation of the square-bracketed term in equation (3) containing the drag coefficient C_{D}:

$$\frac{3}{4}\frac{C_{\mathrm{D}}}{d_{\mathrm{b}}}\rho_{\mathrm{L}} = (\rho_{\mathrm{L}} - \rho_{\mathrm{G}})g\frac{1}{V_{\mathrm{b0}}^2} \quad (4)$$

where V_{b0} is the rise velocity of the bubble swarm at low superficial gas velocities (as indicated by the large filled circle in figure 5). When the superficial gas velocity U is increased, liquid circulations tend to kick in and equation (3) will properly take account of the slip between the gas and liquid phases. Our approach is valid when the bubble size does not increase significantly with increasing U; this is a good approximation for noncoalescing systems but will not hold for air–water. It is important to note that we do not need to know the bubble diameter d_{b} in order to calculate the momentum exchange $\mathbf{M}_{\mathrm{L,G}}$.

For the continuous liquid phase, the turbulent contribution to the stress tensor is evaluated by means of a k–ε model, using standard single-phase parameters $C_\mu = 0.09$, $C_{1\varepsilon} = 1.44$, $C_{2\varepsilon} = 1.92$, $\sigma_k = 1$ and $\sigma_\varepsilon = 1.3$. The applicability of the k–ε model has been considered in detail by Sokolichin and Eigenberger [16]. No turbulence model is used for calculating the velocity fields inside the dispersed bubble phases.

A commercial CFD package CFX, versions 4.2 and 4.4, of AEA Technology, Harwell, UK, was used to solve the equations of continuity and momentum. This package is a finite volume solver, using body-fitted grids. The grids are nonstaggered and all variables are evaluated at the cell centers. An improved version of the Rhie–Chow algorithm [17] is used to calculate the velocity at the cell faces. The pressure–velocity coupling is obtained using the SIMPLEC algorithm [18]. For the convective terms in equations (1) and (2), hybrid differencing was used. A fully implicit backward differencing scheme was used for the time integration.

All simulations were carried out using axisymmetric 2D grids. Simulations were run in columns with diameters of 0.1, 0.19, 0.38 and 6 m, with superficial gas velocities U ranging to 0.20 m/s. The total column height used in the simulations in the 0.1, 0.19 and 0.38 is 1.3 m. For the 6-m diameter column, the total column height is taken to be 35 m. The grids used for the simulations are uniform in both directions; see figure 6(a) and (b). The total number of cells for the 0.1-, 0.19- and 0.38-m diameter columns is 2600. The total number of cells for the 6.0-m diameter column is 26880.

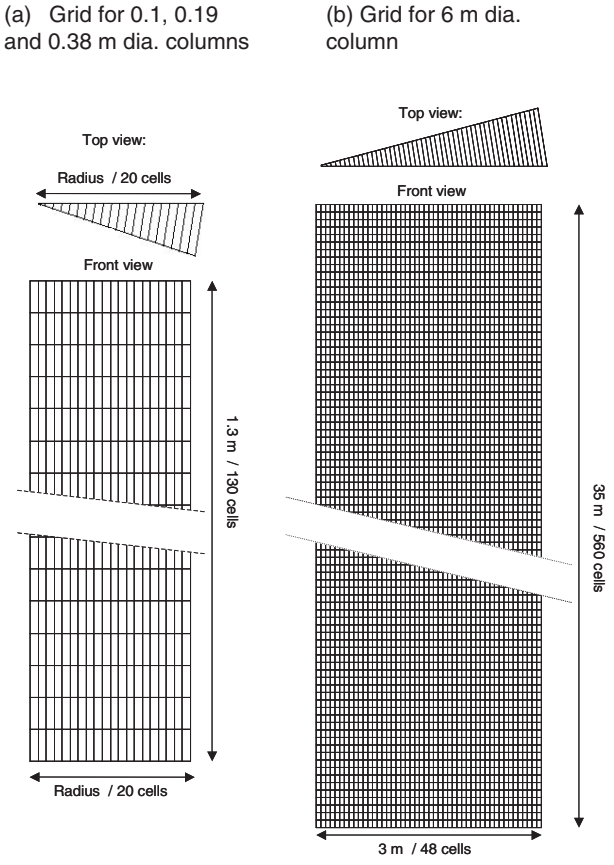

Figure 6. Grid used in the 2D cylindrical axisymmetric Eulerian simulations.

To prevent a circulation pattern in which the liquid flows up near the wall and comes down in the core, the gas was not injected homogeneously over the full bottom area. Instead, the injection of gas was performed on the inner 75% of the radius (15 out of 20 grid cells in the 0.1-, 0.19- and 0.38-m diameter columns and 36 out of the 48 cells in the 6-m diameter column).

A pressure boundary condition was applied to the top of the column. A standard no-slip boundary condition was applied at the wall. The 0.1-, 0.19- and 0.38-m diameter columns were initially filled only with liquid, up to a height of 0.8–1 m, depending on the superficial gas velocity. The initial liquid height for the 6-m diameter columns was 25 m. Transient simulations of the column hydrodynamics were then carried out by imposing a constant superficial gas velocity at the bottom inlet. The time-stepping strategy used in the transient simulations was 100 steps at 5×10^{-5} s, 100 steps at 1×10^{-4} s, 100 steps at 5×10^{-4} s, 100 steps at 1×10^{-3} s, 200 steps at 3×10^{-3} s, 1400 steps at 5×10^{-3} s and the remaining steps until steady state at 1×10^{-2} s. Steady state was obtained when none of the state variables in the system were subject to change.

The simulations were carried out on Silicon Graphics Power Indigo workstation with 75-MHz R8000 processors. Each simulation was completed in about 24 h for the three smaller column diameters. Each of the 6-m column simulations took 4 weeks to complete. When steady state is established, the cumulative gas holdup can be determined along the column height. All the gas holdup data reported in this paper correspond to the cumulative gas holdup at a height of 0.9 m above the distributor for the smaller diameter column and 23 m for the 6-m diameter column.

Further details of the simulations, including animations of column start-up dynamics are available on our website: http://ct-cr4.chem.uva.nl/viscousbc.

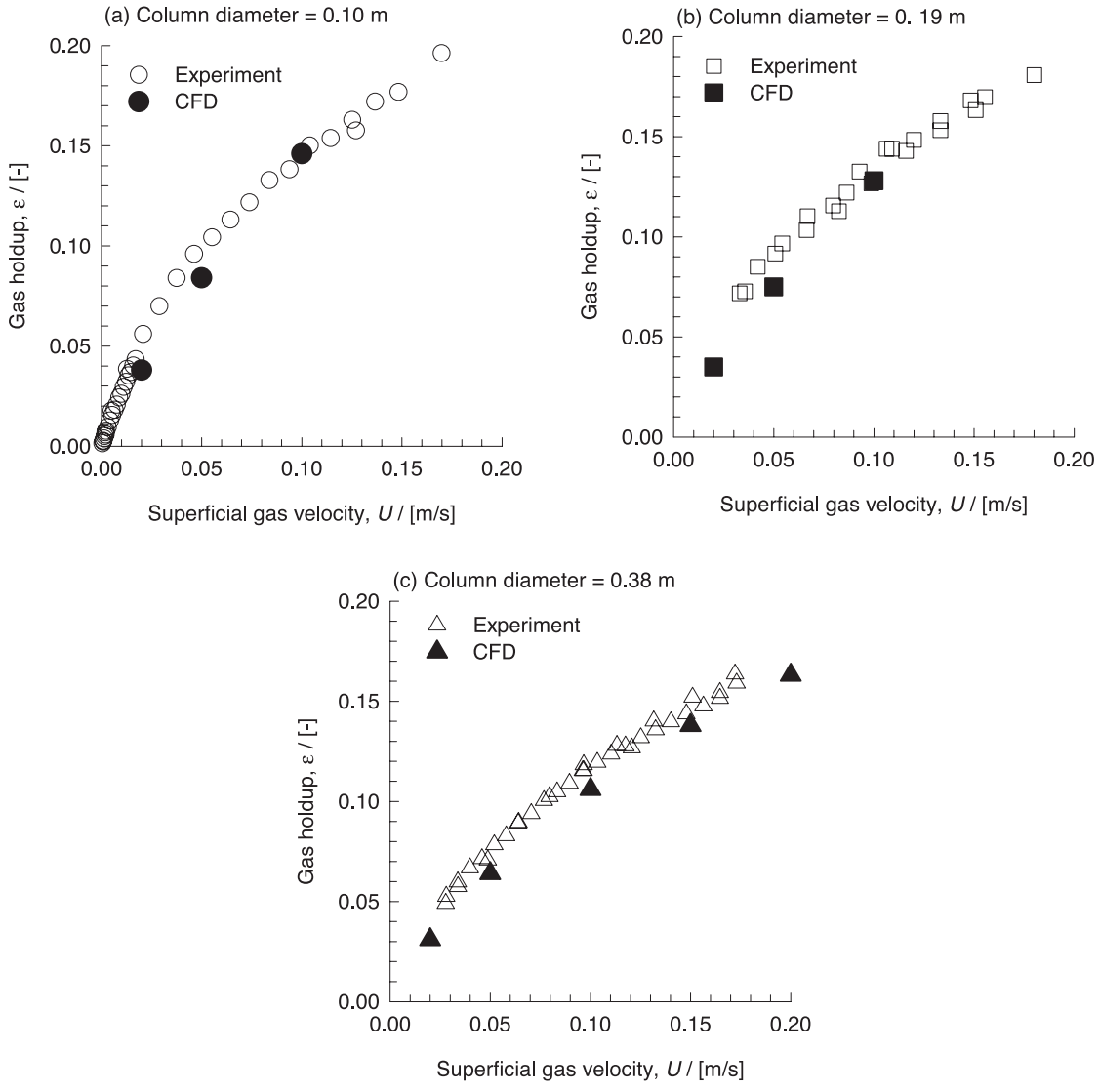

Figure 7. Experimental data on gas holdup as function of the superficial gas velocity U for columns of diameter $D_T = 0.1$, 0.19 and 0.38 m. Comparison with CFD simulations.

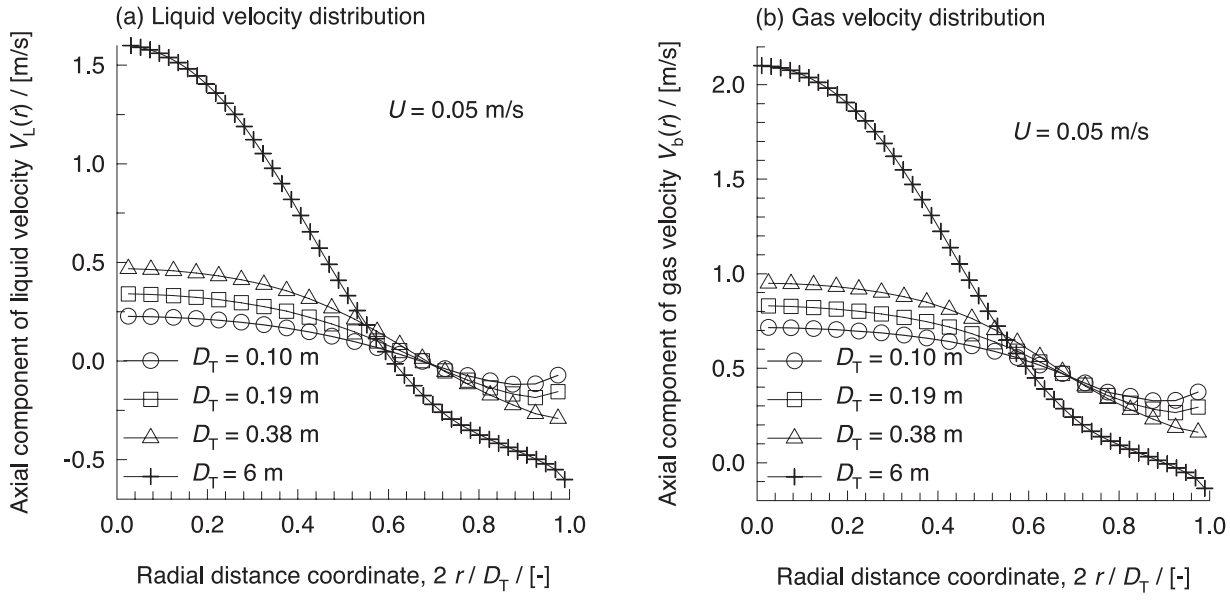

Figure 8. Radial distribution of (a) liquid velocity $V_L(r)$ and (b) gas velocity $V_b(r)$ for varying column diameters for a superficial gas velocity $U = 0.05\,\mathrm{m/s}$.

4. Simulation results for scale influence

The Eulerian simulations for the total gas holdup are compared with the experimental data in figure 7. The agreement is seen to be very good. Clearly, the CFD simulations are able to model the scale effects on the gas holdup. In order to understand scale effects further, we examine the radial distribution of the liquid and gas (bubble) velocities, $V_L(r)$ and $V_b(r)$ in figure 8(a) and (b) respectively for $U = 0.05\,\mathrm{m/s}$. We see from figure 8(a) that the liquid circulation velocities increase strongly with column diameter. At the center of the column, for example, the axial component of the liquid velocity $V_L(0)$ is 0.23 m/s in the 0.1-m diameter column; this value increases to 0.34 m/s in the 0.19-m column and to 0.47 m/s in the 0.38-m column. In the 6-m column, $V_L(0) = 1.6\,\mathrm{m/s}$. Since the drag between the gas bubbles and the liquid is the same for all column diameters, the rise velocity of the bubbles has to increase with increasing column diameter. This is reflected in the axial component of the gas (bubble) velocity, $V_b(r)$, shown in figure 8(b). At the center of the column, for example, the bubble rise velocity $V_b(0)$ is 0.71 m/s in the 0.1-m diameter column; this value increases to 0.83 m/s in the 0.19-m column and to 0.95 m/s in the 0.38-m column. In the 6-m column, $V_b(0) = 2.1\,\mathrm{m/s}$.

The strong influence of column diameter on the gas holdup and the bubble swarm velocity is emphasized in figure 9(a) and (b). We note that the scale effect becomes stronger with increasing superficial gas velocities. Consider operation of the slurry bubble column at $U = 0.15\,\mathrm{m/s}$. In the 0.38-m diameter column, the gas

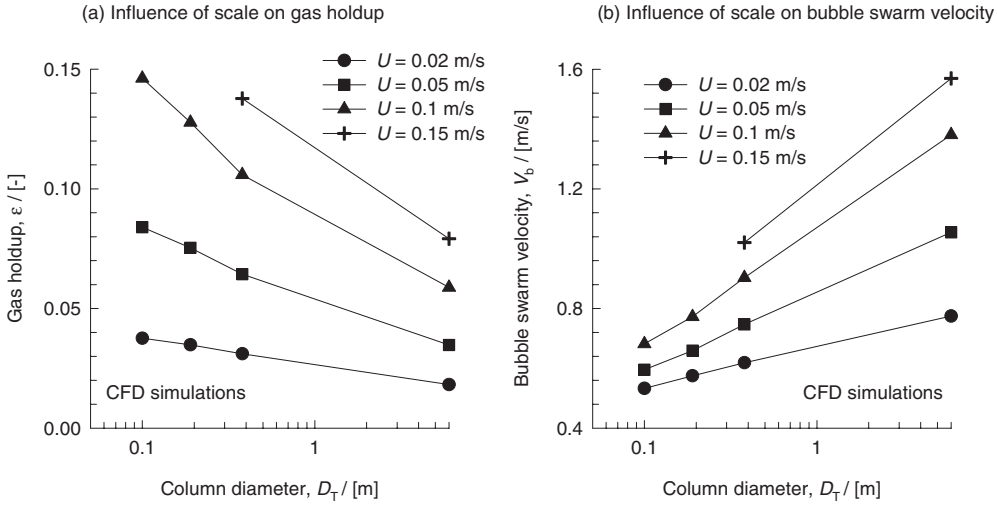

Figure 9. Influence of column diameter on (a) gas holdup and (b) average bubble swarm velocity predicted by CFD simulations.

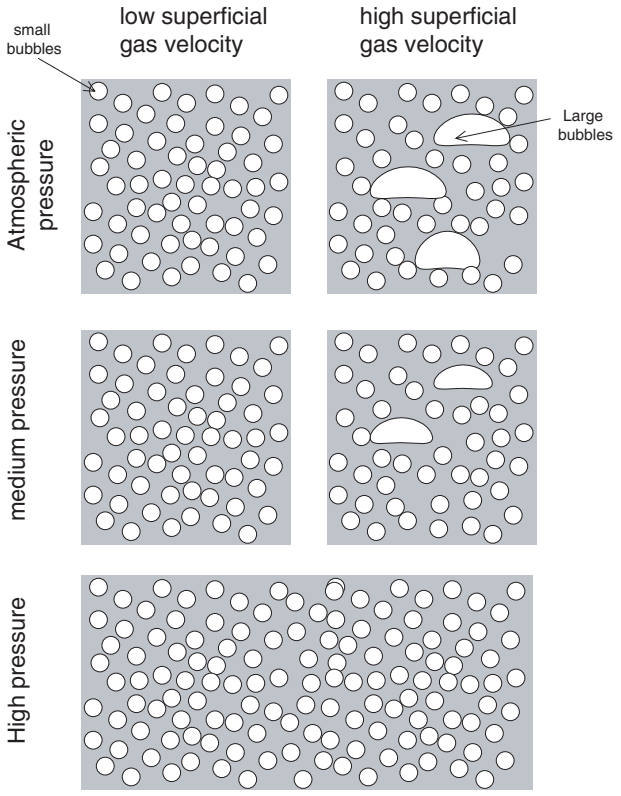

Figure 10. Qualitative picture of the influence of increasing pressure on the hydrodynamics of gas–liquid bubble columns (without the presence of suspended catalyst particles).

holdup is 0.138; this reduces to a value $\varepsilon = 0.079$ in the 6-m diameter column, which amounts to a 40% reduction.

5. Influence of operation at elevated pressures

The FT reactor operates at pressures of around 3–4 MPa. Increasing pressure delays the onset of the heterogeneous flow regime and also reduces the size of the large bubbles [7,19–23]; see the qualitative picture for gas–liquid bubble column operation sketched in figure 10. If the pressure is high enough, the gas dispersion consists of only small bubbles. By comparing figures 3 and 10, we see that the influence of increasing amounts of catalyst particles on the bubble hydrodynamics is opposite to the influence of increasing system pressures. While addition of catalyst particles promotes coalescence and increases the proportion of large bubbles, the influence of increasing pressure is to reduce the population and size of the large bubbles. The prediction of the hydrodynamics of slurry reactors operating at high slurry concentrations and at high pressures is, therefore, particularly difficult. The approach we suggest is to adopt CFD techniques wherein the interphase momentum exchange term is suitably modified to take the pressure effect into account [7].

Nomenclature

C_D	drag coefficient, dimensionless
d_b	diameter of bubble, m
D_T	column diameter, m
g	gravitational acceleration, 9.81 m s^{-2}
g	gravitational vector, m s^{-2}
M	interphase momentum exchange term, N m^3
p	system pressure, Pa
r	radial coordinate, m
t	time, s
u	velocity vector, m s^{-1}
U	superficial gas velocity, m s^{-1}
$V_b(r)$	radial distribution of bubble velocity, m s^{-1}
$V_L(r)$	radial distribution of liquid velocity, m s^{-1}
V_b	cross-sectional area average rise velocity of bubble swarm, m s^{-1}
V_{b0}	bubble rise velocity at low superficial gas velocities, m s^{-1}
$V_L(0)$	centerline liquid velocity, m s^{-1}
Greek	
ε	total gas holdup, dimensionless
μ	viscosity of fluid phase, Pa s
ρ	density of phase, kg m^{-3}
σ	surface tension of liquid phase, N m^{-1}
Subscripts	
b	referring to bubbles
G	referring to gas
L	referring to liquid
T	tower or column
k, l	referring to phase k and l respectively

6. Conclusions

In this paper, we have put forward a scale-up strategy for bubble column slurry reactor for Fischer–Tropsch synthesis using CFD as a pivotal tool. For operation with concentrated slurries, with slurry concentrations in excess of 30 vol%, the dispersion consists almost exclusively of fast-rising large bubbles. By extrapolating the bubble swarm velocity data to low superficial gas velocities, the slip velocity between the bubbles and the slurry phase can be determined. For the 36 vol% paraffin–oil slurry, a value $V_{b0} = 0.47$ m/s is obtained; see figure 5. This value of V_{b0} is used to estimate the drag coefficient C_D between the gas and the slurry phase using equation (4). Eulerian simulations of the slurry bubble column with varying diameters are then carried out by treating the slurry phase as a highly viscous liquid. The CFD simulations are in very good agreement with the experimental results for gas holdup in 0.1-, 0.19- and 0.38-m diameter columns. Simulations for a 6-m diameter column show extremely strong scale dependence, especially for increasing superficial gas velocities.

Once the bubble hydrodynamics have been determined for the commercial scale reactor of, say, 6 m, more reliable estimates can be made of the axial dispersion coefficients, mass and heat transfer coefficients.

Acknowledgment

The Netherlands Organisation for Scientific Research (NWO) is gratefully acknowledged for providing financial assistance in the form of a "programmasubsidie" for development of novel concepts in reactive separations technology.

References

[1] C. Maretto and R. Krishna, Catal. Today 52 (1999) 279.
[2] R. Krishna and J.M. van Baten, Chem. Eng. Technol. 25 (2002) 1015.
[3] R. Krishna, J.M. van Baten, M.I. Urseanu and J. Ellenberger, Chem. Eng. Sci. 56 (2001) 537.
[4] R. Krishna, J.M. van Baten, M.I. Ursenu and J. Ellenberger, Catal. Today 66 (2001) 199.
[5] R. Krishna, J.M. van Baten and M.I. Urseanu, Chem. Eng. Technol. 24 (2001) 451.
[6] R. Krishna and J.M. van Baten, Chem. Eng. Res. Des. 79 (2001) 283.
[7] R. Krishna and J.M. van Baten, Chem. Eng. Sci. 56 (2001) 6249.
[8] R. Krishna, J.M. van Baten and M.I. Urseanu, Chem. Eng. Sci. 55 (2000) 3275.
[9] R. Krishna, Oil Gas Sci. Technol. 55 (2000) 359.
[10] R. Krishna, M.I. Urseanu, J.M. van Baten and J. Ellenberger, Chem. Eng. Sci. 54 (1999) 4903.
[11] J.M. van Baten and R. Krishna, Chem. Eng. Sci. 56 (2001) 503.
[12] R. Krishna, J.W.A. de Swart, J. Ellenberger, G.B. Martina, C. Maretto, AIChE J. 43 (1997) 311.
[13] R. Krishna, M.I. Urseanu, J.W.A. de Swart and J. Ellenberger, Can. J. Chem. Eng. 78 (2000) 442.
[14] Y. Pan, M.P. Dudukovic and M. Chang, Chem. Eng. Sci. 54 (1999) 2481.
[15] J. Sanyal, S. Vasquez, S. Roy and M.P. Dudukovic, Chem. Eng. Sci. 54 (1999) 5071.
[16] A. Sokolichin and G. Eigenberger, Chem. Eng. Sci. 54 (1999) 2273.
[17] C.M. Rhie and W.L. Chow, AIAA J. 21 (1983) 1525.
[18] J. van Doormal and G.D. Raithby, Numer. Heat Transfer 7 (1984) 147.
[19] H.M. Letzel, J.C. Schouten, R. Krishna and C.M. van den Bleek, Chem. Eng. Sci. 52 (1997) 4447.
[20] H.M. Letzel, J.C. Schouten, C.M. van den Bleek and R. Krishna, Chem. Eng. Sci. 52 (1997) 3733.
[21] M.H. Letzel, J.C. Schouten, C.M. van den Bleek and R. Krishna, AIChE J. 44 (1998) 2333.
[22] H.M. Letzel, J.C. Schouten, R. Krishna and C.M. van den Bleek, Chem. Eng. Sci. 54 (1999) 2237.
[23] R. Krishna, M.I. Urseanu and A.J. Dreher, Chem. Eng. Process. 39 (2000) 371.